

High Frequency Piezoelectric Resonant Nanochannel for Bio-Sensing Applications in Liquid Environment

Chiara Zuniga, Matteo Rinaldi and Gianluca Piazza

Department of Electrical and Systems Engineering
University of Pennsylvania
Philadelphia, PA, USA

{zunigac, rinaldim, piazza}@seas.upenn.edu

Abstract—This paper reports on the first demonstration of a 457 MHz AlN Piezoelectric Resonant Nanochannel (PRN) for bio-sensing applications in liquid environment. A novel process consisting of 7 lithographic steps was developed to fabricate the PRN. The new resonant device shows an unchanged value of the electromechanical coupling, k_t^2 (about 0.8 %), whether the channel is filled with air or water and a quality factor, Q , in liquid of approximately 170. The value of k_t^2 and Q are respectively about 2.7 and 2 times the ones recorded for conventional laterally vibrating AlN Contour Mode Resonant Sensors (CMR-Ss) submerged in water. Overall, these results translate in a ~ 5 fold enhancement in the figure of merit ($k_t^2 \cdot Q$ product) of the resonant device when operated in liquid and simultaneously permit the efficient delivery of ultra-low concentrations of fluid samples directly on the surface of the sensor.

I. INTRODUCTION

Lab-on-chip systems are considered an interesting engineering solution that will address issues in public health and welfare by increasing analysis throughput and dramatically reducing reagent cost.

An essential component in the development and miniaturization of lab-on-chip systems is the bio-detector. Acoustic gravimetric sensors, such as Quartz Crystal Microbalances (QCMs), have shown great potentials when employed as bio-detectors [1]. The main advantage of this category of sensors compared to other technologies such as conductance-based sensors (e.g. Chem-FET), or optical sensors, lies in the fact that they use frequency as the output variable, which is one of the physical quantities that can be monitored with the highest accuracy [2]. However, because of their size, QCMs fail to represent a viable solution for lab-on-chip applications that require miniaturized sensors integrated in large arrays.

In recent years, miniaturized devices based on micro and nanoelectromechanical systems (MEMS/NEMS) technology have emerged as a viable response to the need for compact, inexpensive and integrable resonant sensors. Their reduced mass allows them to achieve unprecedented levels of

resolution [3] and makes them suitable for detecting minuscule concentrations of target analyte in bio-samples.

However, when M/NEMS resonant sensors are required to operate in a liquid environment (typical of bio-applications), additional challenges need to be overcome in order to achieve the same levels of performance shown in air.

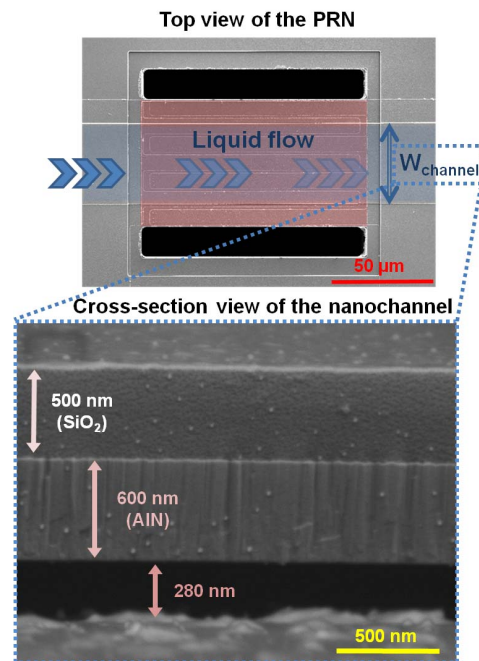


Figure 1. Scanning Electron Microscopy (SEM) images of the PRN sensor and the nanochannel cross-section. It is worth noting that the silicon dioxide layer is not present on top of the resonant section (solely formed by AlN), but exclusively on the portion of the channel that leads to the inlet and outlet of the resonator.

The operation of acoustic gravimetric sensors in liquid environment is in fact degraded by the viscous force acting on the resonator surface, which causes energy radiation in the surrounding media and consequently decreases the device

quality factor, Q , and its frequency resolution. In addition the immersion of the resonant device in the liquid media renders its transduction more challenging and less efficient, which translates in the need of cumbersome and power consuming actuation and readout techniques. Although there have been demonstrations of bio-detection via mass sensing in miniaturized resonators such as cantilever beams [4], these prototypes have experienced reduced performance compared to operation in air or vacuum, and suffered from the lack of an adequate fluidic system for the delivery of the bio-samples in a small volume and in direct contact with the surface of the resonant device.

The integration of a microfluidic channel inside the body of a resonant cantilever beam sensor [3] has been proposed as a solution to simultaneously address the issue of viscous damping and realizing a compact delivery system that reduces sample volume. Although highly effective in maintaining unaltered mechanical performances, these hollow cantilever beams required a high DC voltage (as high as 120 V [3]) for their electrostatic actuation and a cumbersome and power inefficient optical readout. In addition, the reduced frequency of operation (few 100s of KHz) limited the device sensitivity and ultimate resolution for certain applications.

Recently, the capability to fabricate higher frequency (100 MHz - 10 GHz) [5] resonant sensors with ultra-low values of limit of detection (LOD) in air [6, 7] has been demonstrated employing the Nanoscaled AlN Contour Mode Resonant Sensor (CMR-S) technology.

In this work, for the first time, a Piezoelectric Resonant Nanochannel Sensor is proposed as an innovative solution for the realization of resonant bio-sensor devices with high frequency of operation, reduced viscous damping, improved transduction efficiency and effective delivery of the bio-sample solely on the active sensing surface of the device. By transforming the resonant body of the CMR into a laterally vibrating nanochannel, the thickness of the viscous layer as well as the total amount of liquid in contact with the resonator surface has been reduced. Therefore, the new device achieves a 5 fold enhancement in the figure of merit ($k_t^2 \cdot Q$, product of the electromechanical coupling and resonator Q) with respect to a conventional CMR-S and results in an unchanged k_t^2 (approximately 0.8 %) with respect to the measurement in air and a Q in fluid of approximately 170. Furthermore, the novel layout permits the delivery of the fluid solely and in close proximity of the sensing surface (which can also be doubled with respect to the conventional CMR-S), therefore resulting in a greatly improved device-sample interaction.

II. DESIGN

An efficient method for the delivery of the bio-sample onto the resonant element is ultimately of crucial importance in determining the overall performance of a resonant bio-sensor. In fact, if the resonator were to be immersed in a large volume of the fluid sample, it would not be statistically able to interact with some of the very low concentration analytes contained in the sample itself. Therefore, a major fraction of the analyte would be exhausted without contributing to the detection process [8].

In this perspective, the implementation of a high surface to volume ratio resonant nanochannel represents the optimum design solution, since it allows confining a small sample volume (pL) in a thin layer proportional to the penetration depth of the acoustic wave (*i.e.* closely in contact with the entire vibrating structure), reducing viscous drag and maximizing the sample-device interaction.

Simultaneously, the design choice of forming a resonant nanochannel solves another issue related to the transduction efficiency of nanoscale structures in liquids. The PRN confines the electric energy (necessary for actuation) in the piezoelectric body of the device minimizing energy leak into the fluid. In fact, if a conventional CMR-S were simply immersed in a large volume of fluid, most of the electrical energy would be confined in the fluid rather than the resonator body due to the higher dielectric constant of the fluid with respect to the AlN piezoelectric film.

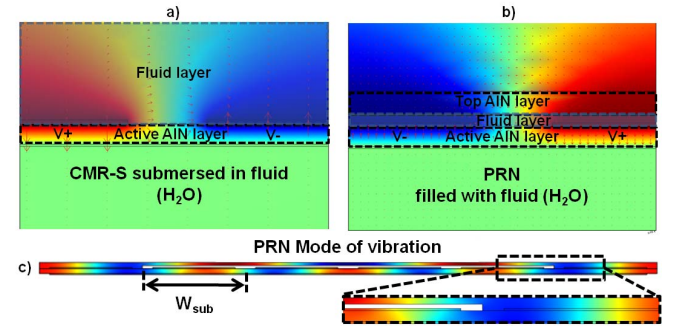


Figure 2. (a) Zoomed in view (two adjacent electrodes) of FEM simulation results for the electric potential (colors) and electric field (arrows) distribution in a conventional CMR-S. (b) and a Piezoelectric Resonant Nanochannel (PRN). (c) displays the mode of vibration of the PRN, highlighting that the entire body of the channel is actually vibrating at the prescribed resonance frequency (set by W_{sub}).

The beneficial effect that the design of a resonant nanochannel has on the confinement of electrical energy in the resonant device and consequently on its electromechanical coupling coefficient is confirmed by 2D electrostatic Finite Element Method (FEM) analysis performed using COMSOL Multiphysics 3.5 – Electrostatic AC/DC Module. As shown in Table I, the presence of fluid (set to be water in the analysis) is such that most of the electrical energy is confined in the fluid rather than the resonator when a conventional CMR-S is used. When instead the PRN is employed, most of the electrical energy is effectively stored in the piezoelectric (active) body of the device rather than the liquid media.

This beneficial effect on the device electrical performance can be alternatively seen as a reduction in the parasitic capacitance introduced by the liquid media. In fact, the presence of water introduces a large parasitic capacitance, C_p (~ 680 fF), in parallel to the device geometrical capacitance, C_0 , which, as highlighted in [9], negatively affects the k_t^2 of the device ($k_t^2 \propto C_m/C_0$). It is possible to observe (Table I) that, when the PRN is employed, the value of such parasitic parallel capacitance, C_p , is significantly reduced ($C_p \sim 38$ fF) and negligible if compared to the device capacitance, C_0 .

Based on these considerations, the PRN is designed to have a nanoscaled channel depth of 280 nm. The device is formed by two AlN layers, 500 nm and 600 nm thick respectively, separated by an air gap of 280 nm.

TABLE I. COMSOL FEM SIMULATIONS OF DEVICE ELECTROSTATICS

FEM Simulations	CMR-S	CMR-S w/ top AlN	PNR-S
C_0 - Geometrical	244 fF	267 fF	260 fF
C_p - Parasitic in H_2O	682 fF	173 fF	38 fF
C_{tot} - Total capacitance in H_2O	926 fF	440 fF	298 fF
Energy density stored in device	1.01 $nJ/m \cdot V^2$	1.01 $nJ/m \cdot V^2$	1.04 $nJ/m \cdot V^2$
Energy density dissipated in H_2O	1.74 $nJ/m \cdot V^2$	0.67 $nJ/m \cdot V^2$	0.174 $nJ/m \cdot V^2$

The first AlN layer (active layer, 500 nm) is actively transduced (piezoelectrically) to generate vibration in the PRN, while the second AlN layer (structural layer, 600 nm) is used to form the top surface of the resonant nanochannel. Similarly to conventional CMR-S [6], the resonance frequency of the PRN is approximately set by the width, W_{sub} , of an individual device finger (Fig. 2-c) and the equivalent acoustic velocity of the material stack forming the resonator. The active AlN layer of the PRN of this work is formed of 6 fingers ($n=6$) whose width, W_{sub} , is set to be 10 μm . This configuration translates in a frequency of operation of 457 MHz ($\sim 1000X$ higher than the one achieved by Suspended Nanochannel Resonators [3]). The total width of the PRN is 60 μm with an effective nanochannel width of 40 μm . The total length of the channel (from inlet to outlet) is 4.1 mm. Therefore, the nanochannel occupies a surface area of 60,000 μm^2 and an overall volume of 46 pL. The device active region (which undergoes mechanical vibrations) occupies a surface area of 4,800 μm^2 and an overall volume of only 1.34 pL.

III. FABRICATION PROCESS

The wafer level integration of the 280 nm AlN resonant-nanochannel was realized through a 7 mask fabrication (Fig.3) by adding 3 lithographic steps to the standard process developed for CMR-S [6].

Optical lithography was first performed for the definition of the bottom floating Pt plate (50 nm) sputtered on a high resistivity Si substrate. This step was followed by sputter deposition of c-axis piezoelectric AlN thin (500nm) film (Fig.3-a). This first layer of the AlN represents the active piezoelectric film that is sandwiched between the two metal layers; however, the entire structure forming the PRN is excited into lateral vibration as shown in Fig.2-c.

The top Pt layer (50 nm) was deposited by evaporation and patterned by a lift-off process (Fig.3-b). A very thin film (~ 15 nm) of Plasma Enhanced Chemical Vapor Deposition

(PECVD) deposited silicon dioxide (SiO_2) was placed onto the device top surface to enhance the adhesion between Pt and the subsequent layer of amorphous silicon (a-Si).

a-Si (280 nm thick) was then evaporated and patterned through reactive ion etching (RIE) in SF_6 chemistry to define the shape of the nanochannel (Fig.3-c). A second layer of AlN (600 nm thick) was sputtered on the patterned sacrificial layer to form the top encapsulation of the resonant nanofluidic channel (Fig.3-d). Wet etch in phosphoric acid (H_3PO_4) at 150 $^\circ C$ was employed to open vias in the top AlN layer in order to access the pads for the electrical connections to the device (Fig.3-e).

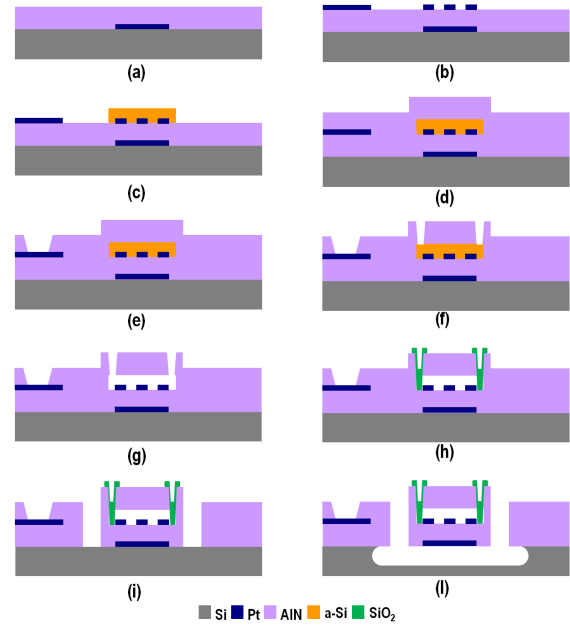


Figure 3. Fabrication process of the PRN. The process requires 3 additional lithographic steps with respect to the standard fabrication of CMR.

In order to remove the amorphous silicon sacrificial layer and to form the inlet/outlet openings of the nanochannel, 100 x 100 μm etch holes were defined on the top AlN layer at the extremities of the channel by inductively coupled plasma (ICP) dry etching. Simultaneously, small holes (5x10 μm) were periodically defined along the length of the channel in order to more efficiently remove the amorphous silicon (Fig.3-f).

The nanochannel was released by dry etching of the amorphous Silicon in XeF_2 (Fig.3-g). Subsequently the small holes (used to etch it) were sealed through a 500 nm thick SiO_2 layer deposited by PECVD. This layer of oxide was removed (by CH_6 chemistry RIE) only from the body of the device, the pads for the electrical connections as well as the inlet/outlet of the nanochannel (Fig.3-h).

Lastly, the body of the resonator was defined by ICP dry etching of the two AlN layers and the PRN was released from the substrate by XeF_2 isotropic dry etching of silicon as shown in Fig.3-i,l.

IV. EXPERIMENTAL RESULTS

The performance of the 457 MHz AIN Piezoelectric Resonant Nanochannel were evaluated by testing the device in an RF probe station and recorded by an Agilent PNA N5230A network analyzer. Its electrical response with and without any liquid filling the channel was characterized and its equivalent electrical parameters were extracted by fitting the admittance curves to a MBVD model [10].

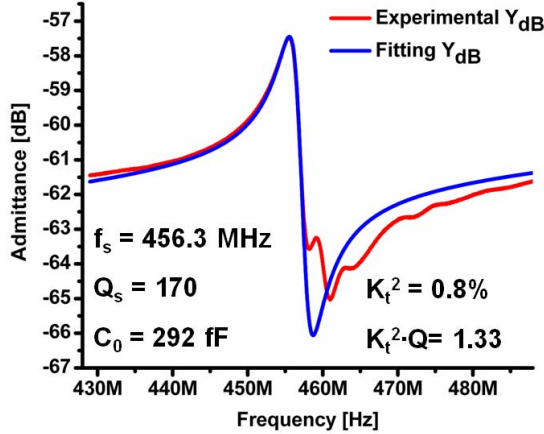


Figure 4. Electrical response of the 457 MHz PRN with de-ionized water filling the nanochannel and in ambient conditions.

In order to test the device response in a viscous environment, a drop of $\sim 1 \mu\text{L}$ of de-ionized water was dispensed through a micropipette on top of one of the inlets of the nanochannel: as a result, part of the drop (46 pL is the total volume of the channel) was sucked inside the nanofluidic channel by capillary forces and a difference in the density of the viscous fluid (going from air to water) was recorded by the device. The device experienced a drop in Q (with respect to air) because of the additional damping introduced by the liquid media confined in its body. A quality factor in liquid equal to 170 was achieved proving that delivering a reduced thickness of the viscous layer as well as a smaller total amount of liquid in contact with the resonator surface determines a 2 X enhancement in the device quality factor. The extracted experimental data are summarized in Table II, where the PRN is compared to a CMR device of identical total thickness ($1.1 \mu\text{m}$) that was fabricated at the same time side to side to the PRN, but without the airgap forming the resonant nanochannel.

Despite the decrease in quality factor, the electromechanical coupling coefficient of the PRN remained unaltered and equal to 0.8% proving that the confinement of the fluid is advantageous in reducing the parasitic capacitance in parallel with the device and improving the resonator transduction efficiency. This result directly relates to a better confinement of the electric energy in the AIN body of the resonator and is in line with the FEM predictions.

TABLE II. SUMMARY OF EXPERIMENTAL RESULTS

		f_0 [MHz]	Q	C_0	k_t^2	$k_t^{2*}Q$
PRN	Air	457.9	1082	278	0.83%	9.13
	H ₂ O	456.3	170	292	0.80%	1.33
CMR-S w/ top AIN	Air	460.7	961	306.5	0.97%	9.36
	H ₂ O	458.6	90	478	0.29%	0.26

Differently, the conventional CMR suffered from a more damped response when immersed in liquid (Q of 90), and a less efficient transduction ($k_t^2 \sim 0.29\%$) due to the large parasitic capacitance introduced by the liquid media.

V. CONCLUSIONS

In this work, for the first time, a high frequency (457 MHz) Piezoelectric Resonant Nanochannel for operation in liquid media was demonstrated. This new device shows an unchanged value of k_t^2 (0.8%) whether the channel is filled with air or water and a Q in liquid of approximately 170, which translates in a 5 X enhancement in performance with respect to a conventional CMR-S submerged in liquid media. This innovative solution for the realization of resonant bio-sensor devices combines a high frequency of operation (1000 X higher than cantilever beams) and the capability to employ efficient on chip actuation and sensing of the device, therefore enabling the use of a compact and low power electronic readout. Additionally, because of the unique capability of arraying large number of PRNs with different frequencies of operation in a small footprint, this novel technology lays the foundation towards the demonstration of large arrays of Piezoelectric Resonant Nanochannels for highly multiplexed bio-sensing applications that require high throughput and reduced sample volume.

REFERENCES

- [1] L. Arce, M. Zougagh, C. Arce, A. Moreno, A. Rios, M. Valcarcel, *Biosensors and Bioelectronics* 22 (2007) pp. 3217–3223.
- [2] J. R. Vig, L. Filler, Y. Kim, *J. Microelectromech. Syst.*, vol. 5, no. 2, pp. 131–137, 1996.
- [3] Jungchul Lee, Wenjiang Shen, Kris Payer, Thomas P. Burg, and Scott R. Manalis, *Nano Lett.* 2010, 10, 2537–2542.
- [4] M. Yue, J. C. Stachowiak, H. Lin, R. Datar, R. Cote and A. Majumdar, *Nano Lett.*, 2008, 8 (2), pp 520–524.
- [5] M. Rinaldi, C. Zuniga, and G. Piazza, *Proc. 22nd IEEE International Conference on Micro Electro Mechanical Systems (MEMS 2009)*, Sorrento, Italy, Jan. 2009, pp. 916–919.
- [6] M. Rinaldi, B. Duick, C. Zuniga, C. Zuo and G. Piazza, *Proc. 23rd IEEE International Conference on Micro Electro Mechanical Systems (MEMS 2010)*, pp. 132–135.
- [7] M. Rinaldi, C. Zuniga, C. Zuo and G. Piazza, *Proc. Solid-State Sensors, Actuators, and Microsystems Workshop (Hilton Head 2010)*, Jun. 2010, pp. 471–474.
- [8] G. Wingqvist, J. Bjurström, A.-C. Hellgren, I. Katardjiev, *Sensors and Actuators B* 127 (2007) 248–252.
- [9] M. Rinaldi, C. Zuniga, C. Zuo and G. Piazza, *IEEE Transactions on Ultrasonics, Ferroelectrics, and Freq. Control*, Vol.57 No.1, Jan. 2010, pp 82–87.
- [10] J.D. Larson, P.D. Bradley, S. Wartenberg, and R.C. Ruby, *Proc. IEEE Ultrason. Symp.*, Oct. 2000, pp.863–868.